

# **The Correlated Electronic States of a few Polycyclic Aromatic Hydrocarbons: A Computational Study**

Geetanjali Giri, Y. Anusooya Pati, and S. Ramasesha\*

*Solid State and Structural Chemistry Unit, Indian Institute of Science, Bangalore 560 012, India*

E-mail: ramasesh@sscu.iisc.ernet.in

## Abstract

In recent years Polycyclic Aromatic Hydrocarbons (PAHs) have been studied for their electronic properties as they are viewed as nanodots of graphene. They have also been of interest as functional molecules for applications such as light emitting diodes and solar cells. Since last few years varying structural and chemical properties corresponding to the size and geometry of these molecules have been studied both theoretically and experimentally. In this paper, we carry out a systematic study of the electronic states of several PAHs using the Pariser-Parr-Pople model which incorporates long-range electron correlations. In all the molecules studied by us, we find that the 2A state is below the 1B state and hence none of them will be fluorescent in the gaseous phase. The singlet-triplet gap is more than one-half of the singlet-singlet gap in all cases and hence none of these PAHs can be candidates for improved solar cell efficiencies in a singlet fission. We discuss in detail the properties of the electronic states which include bond orders and spin densities (in triplets) of these systems.

## Introduction

Electronic structure of  $\pi$ -conjugated carbon systems is of enduring interest, although there have been paradigm shifts in the underlying reasons. Early interest revolved around aromaticity<sup>1-3</sup> and later with the advent of the era of electronic polymers, the interest has shifted to the study of relative energy level ordering of the low energy excited states. With recent focus on graphene, there has been a resurgence of interest in condensed aromatic ring systems. Thus, polycyclic aromatic hydrocarbons (PAHs) which were studied mainly for environmental impact are now of interest from the electronic structure view point as these molecules serve as model nanodots of graphene.<sup>4-6</sup> The effect of shape on the optical properties of nanodots of graphene, have also been studied.<sup>7</sup> The role of size, shape and hetero atom doping on the magnetic and electronic properties of graphene quantum dots have been studied theoretically using density functional methods.<sup>8-10</sup> Indeed, it has also been reported that alkali metal doped

picene exhibits superconductivity below 18K<sup>11</sup> and K-doped 1,2:8,9-dibenzopentacene shows superconductivity above 30 K,<sup>12</sup> Sm-doped phenacenes show very low  $T_c \approx 5\text{K}$ ,<sup>13,14</sup> which adds further dimension to the study of PAHs. The spectra of PAHs have also been studied extensively, since they have been detected in the interstellar medium.<sup>15</sup>

Experimental studies have mainly focused on the vibrational spectra of PAH molecules. Allamandola et al have assigned the unidentified infrared bands (UIBs) of interstellar particles to Raman spectra of partially hydrogenated, positively charged PAHs.<sup>16</sup> They have studied the infrared fluorescence spectrum of chrysene molecule. The observation of diffused interstellar absorption bands (DIBs) is attributed to the presence of larger PAHs molecule.<sup>17</sup> Salama et al have obtained the spectra of several neutral and ionic PAH molecules under the astrophysical laboratory conditions and compared this with the astronomical spectra.<sup>18</sup> These astronomical bands can be explained with electronic absorptions and/or dynamical methods such as electronic relaxations and intramolecular vibrational relaxations. Palewska et al have obtained the high resolution fluorescence and phosphorescence spectra of tetrahelicene and hexahelicene in n-heptane matrix at room temperature.<sup>19</sup> They find the singlet-singlet transition to be at 3.1 eV whereas the singlet-triplet transition to be at 2.5 eV. The electronic absorption spectrum of chrysene molecule in boric acid glass matrix is reported by Hussain.<sup>20</sup> They compared their excitation energies obtained from experiments with those obtained from semiempirical AM1 method. They found a reasonably good agreement in the calculated bond lengths and bond angles with those obtained from the X-ray diffraction.

Electronic absorption spectra in complex PAH molecules were obtained within semiempirical approach where restricted configuration interactions were used.<sup>21</sup> Ping Du et al used semi empirical quantum mechanical intermediate neglect of differential overlap (INDO) method to compare optical spectra of naphthalene and its ions with experimental data.<sup>22</sup> Infrared spectra of neutral and cationic PAHs are obtained within the DFT method and the neutral molecules showed a good agreement with the experimental spectra.<sup>23</sup> The absolute absorption cross-

section of several PAH molecules and their cations were obtained within time-dependent density functional theory.<sup>24</sup> They find good agreement with the experimental excitation energies for neutral PAH molecules. This is not surprising as TDDFT method with adiabatic local density approximation is equivalent to single CI method<sup>25</sup> which has been shown to give good optical gaps due to cancellation of errors. However, with ions, this cancellation does not occur. Using time dependent DFT, Hammonds et al have obtained the electronic spectra of protonated and partially hydrogenated PAHs and found similarity in the absorption peaks of diffuse interstellar bands.<sup>26</sup> Size and geometry dependence of larger PAH molecules on optical spectra has been studied by Cocchi et al within ZINDO model, using only single excitation configuration interactions (SCI).<sup>27</sup> The role of aliphatic side groups on the vibrational spectra of PAHs molecule is studied using the DFT method.<sup>28</sup>

A feature common to all conjugated carbon systems is that the  $\pi$ -electrons experience strong correlations. The role of electron correlation on the ordering of the excited state energy levels in PAHs has been studied by Mazumdar et al using Pariser-Parr-Pople model hamiltonian.<sup>29</sup> They find that the effect of electron-electron interactions is weaker in PAHs than in polyenes, but stronger than in the quasi-1D systems like poly-(paraphenylene) and poly-(paraphenylenevinylene). Basak et al have carried out a detailed study of the linear absorption spectra of diamond shaped graphene quantum dots (where pyrene is the smallest unit), with quadruple CI and MRSDCI basis using the correlated PPP model Hamiltonian. They have compared their excitation gaps with screened and standard PPP parameters for carbon.<sup>30</sup> They have also studied the two-photon absorption and photoinduced absorption of these molecules. They find that the effect of electron-electron correlation gets enhanced with the increase in the size of graphene quantum dots.<sup>31</sup> Motivated by this large number of experimental and theoretical data on PAHs, the current study focuses on the effect of strong electron-electron correlations on one-photon and two-photon absorptions in PAHs. So far, a thorough study of this class of molecules inclusive of strong long range electron-electron correlations has not been reported to

the best of our knowledge.

In this paper, we have compared electronic spectra of various PAHs (see Fig. 1) such as Fluoranthene, Pyrene (both 16 conjugated carbon atoms), Benzanthracene, Chrysene, Helicene, Triphenylene (18 conjugated carbon atoms), Benzopyrene (20 conjugated carbon atoms) and Picene (22 conjugated carbon atoms) using numerically exact diagrammatic valence bond (DVB) method as well as Density matrix renormalization group method (DMRG) for larger molecules. We have analyzed the bond orders and spin densities in triplet states based on the ring orientations of these systems. We find that none of the molecules belonging to this class, studied by us, fulfill the energy criterion for singlet fission. Details of methods used in this study are discussed in next section followed by a description of singlet and triplet states of all molecules considered, with their corresponding properties. We have summarized our findings in the last section.

## Methodology

We have considered all molecules to be geometrically planar. Ignoring hydrogen atoms in a molecule leaves us with the carbon skeleton. Carbon atoms in  $sp^2$  hybridization in aromatic hydrocarbons provides three sigma bonds with neighboring atoms resulting in a rigid framework of the system whereas  $2p_z$  orbital gives conjugated network perpendicular to the plane of the molecule. This conjugated framework in aromatic systems gives rise to many interesting properties owing to the delocalized nature of orbitals. In our studies we focus on  $\pi$ -electron network to explore various properties of the PAHs as this network is energetically well separated from the underlying  $\sigma$ -network. This approximation is the  $\sigma - \pi$  separability approximation.<sup>32</sup> In the present study, we have used Pariser-Parr-Pople (PPP) model Hamiltonian to describe the  $\pi$ -electrons.<sup>33,34</sup> PPP model is obtained from many-body Hamiltonian considering only  $\pi$ -electrons and invoking zero differential overlap (ZDO) approximation. The PPP Hamiltonian is

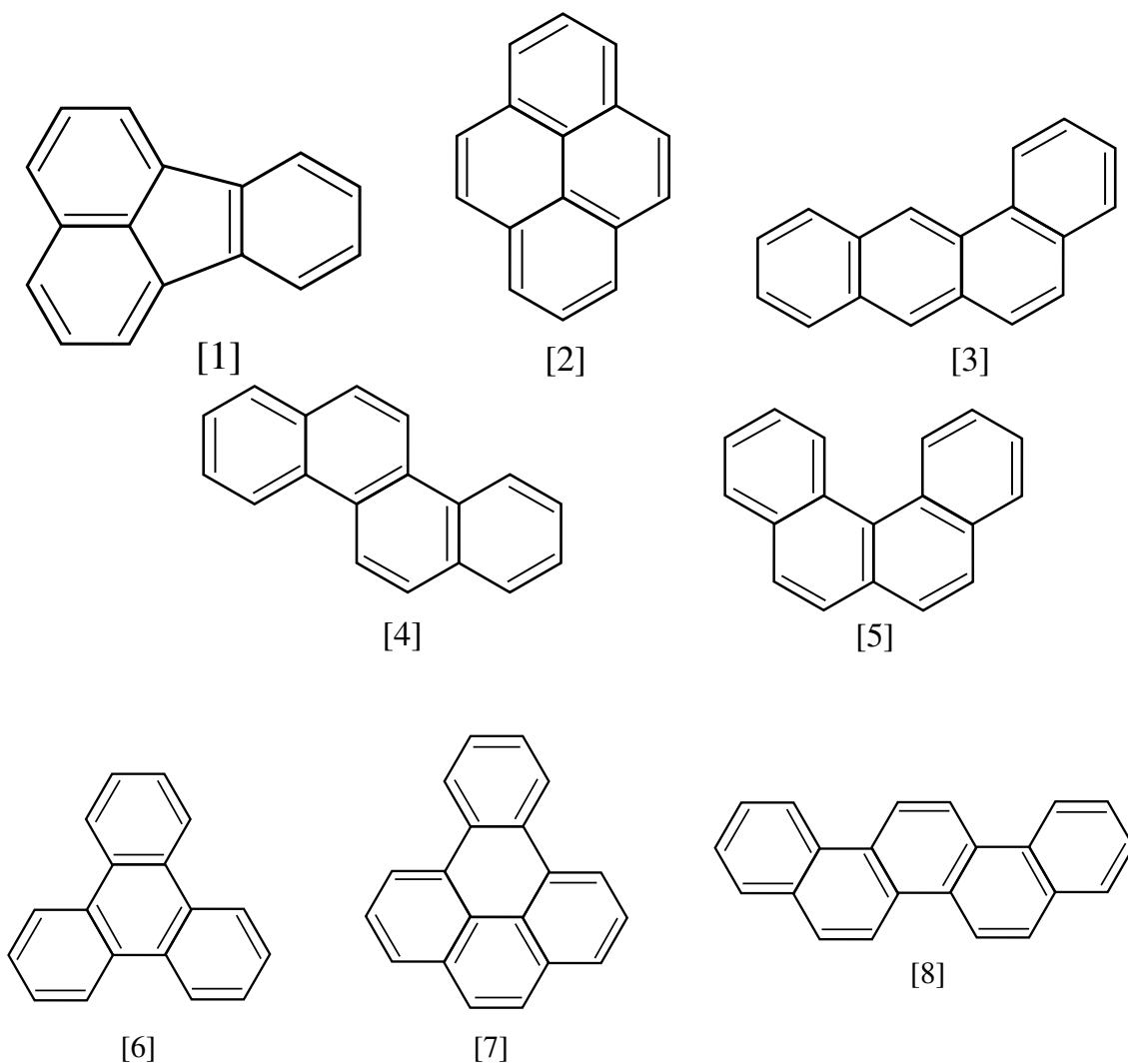


Figure 1: Schematic representation of PAH molecules that have been studied. 1) Fluoranthene, 2) Pyrene, 3) Benzanthracene, 4) Chrysene, 5) Helicene, 6) Triphenylene, 7) Benzopyrene and 8) Picene.

given below:

$$\begin{aligned} \hat{H}_{PPP} = & \sum_{\langle ij \rangle, \sigma} t_0 (\hat{c}_{i,\sigma}^\dagger \hat{c}_{j,\sigma} + H.C.) + \sum_i \varepsilon_i \hat{n}_i \\ & + \sum_i \frac{U}{2} \hat{n}_i (\hat{n}_i - 1) + \sum_{i>j} V_{ij} (\hat{n}_i - z_i) (\hat{n}_j - z_j) \end{aligned} \quad (1)$$

Here first term is the noninteracting part of the PPP Hamiltonian in which  $t_0$  is nearest-neighbour hopping term between two bonded orbitals 'i' and 'j'.  $\hat{c}_{i,\sigma}^\dagger$  ( $\hat{c}_{i,\sigma}$ ) creates (annihilates) an electron of spin  $\sigma$  in  $2p_z$  orbital of carbon atom at site i.  $\varepsilon_i$  is the site energy of 'i'-th carbon atom. The second term corresponds to interacting part of the Hamiltonian which consists of on-site Hubbard repulsion term for two electrons occupying the same orbital. In the third term  $V_{ij}$ s are electron-electron repulsion integrals between electrons in two separate orbitals i and j.  $V_{ij}$ s are interpolated between U and  $\frac{e^2}{r}$  as  $r_{ij} \rightarrow \infty$  using the Ohno interpolation scheme,<sup>35</sup>

$$V_{ij} = 14.397 \left[ \left\{ \frac{28.794}{(U_i + U_j)} \right\}^2 + r_{ij}^2 \right]^{-\frac{1}{2}} \quad (2)$$

The operator  $\hat{n}_i$  is the number operator, the C-C bond length is fixed at 1.4 Å for nearest neighbour carbon atoms. We use the standard PPP model parameters for carbon, namely,  $t_0 = -2.4$  eV,  $U = 11.26$  eV and site energies  $\varepsilon_i = 0.0$  eV for unsubstituted carbon site.  $z_i$  is the number of electrons at site 'i' which leaves the site neutral and correspond to local chemical potential. For carbon atoms in conjugation,  $z_i$  values are set to 1.

The PPP model Hamiltonian conserves total spin. So, to obtain the eigenstates of PAHs within PPP model we have used the diagrammatic valence bond (DVB) method because it generates spin-adapted basis functions contrary to slater basis functions which conserves only the z-component of total spin. To reduce the computational cost further, we have exploited the combination of  $C_2$  and electron-hole (e-h) symmetry and factorized the Hilbert space into sym-

metry adapted bases.<sup>36,37</sup> Since  $C_2$  and eh symmetry operators commute, we have an Abelian group with 4 one-dimensional representation. Except benzenanthracene, all molecules studied by us have  $C_2$  symmetry - either along X-axis or along Y-axis. Since these molecules are assumed to be planar, inversion symmetry and  $C_2$  along Z-axis are equivalent. So, we have also used the term  $C_2$  for inversion symmetry. The space with character +1 under  $C_2$  and +1 under e-h symmetry corresponds to the  $A^+$  space and contains covalent VB diagrams, i.e. VB diagram in which every site is neutral. The ground state of the system is found in this space. The optically connected excited state (to the ground state) is found in the  $B^-$  space, where the character under both  $C_2$  and e-h symmetry is -1. This space does not contain any covalent VB diagram and hence is also called the ionic space. The e-h symmetry exists only in bipartite lattices where the transfer term is nonzero only between atoms in different sublattices. Among the PAHs we have studied only Fluoranthene does not belong to this class. We use the symmetry adapted VB basis to set-up the Hamiltonian matrix.<sup>38</sup> A few low-lying states in each subspace are obtained from the Rettrup algorithm.<sup>39</sup> With the computational resources we have, we can do exact calculations for the singlets when both  $C_2$  and eh symmetries exist, for a system with 20 carbon atoms and 20 electrons (neutral system). The dimensionalities of the subspaces for all the PAH systems we have studied is given in Table 1. Wherever we are unable to carry out exact calculations, we have resorted to the DMRG calculations. Thus triplets of benzopyrene and both singlets and triplets of picene were obtained within the DMRG approach. After obtaining the low-lying eigenstates, to fully characterize the state, we have computed the transition dipole between ground and excited states in appropriate spaces. We have also computed bond orders to understand the nature of equilibrium geometry in all eigenstates. In triplet states we have computed spin densities which can be verified from ESR studies.



**Table 1: Dimensionalities of the symmetry adapted spaces for PAHs studied in this paper. The total number of bases in singlet and triplet spaces for neutral systems with  $N = 16$  are 34,763,300 and 66,745,536; with  $N = 18$  are 449,141,836 and 901,995,588; with  $N = 20$  are 5,924,217,936 and 12,342,120,700; with  $N = 22$  are 79,483,257,303 and 170,724,392,916, respectively.**

Molecule	$N_e = N$	Singlets		Triplets	
		$\mathbf{A}^{\text{cov}}$	$\mathbf{B}^{\text{ionic}}$	$\mathbf{B}^{\text{cov}}$	$\mathbf{A}^{\text{ionic}}$
Pyrene	16	8,698,485	8,695,320	16,692,888	16,689,604
Benzantracene	18	224,573,349	224,568,487	451,003,761	450,991,827
Chrysene	18	112,313,738	112,303,369	225,524,745	225,510,840
Helicene	18	224,573,349	224,568,487	451,003,761	450,991,827
Triphenylene	18	112,313,738	112,303,369	225,524,745	225,510,840
BenzoPyrene	20	1,481,162,738	1,481,122,588	-	-

## Results and Discussion

All the molecules studied, with the exception of fluoranthene, have electron-hole symmetry. Thus the states in these molecules (except fluoranthene) can be classified as 'covalent' ('+') or 'ionic' ('-'). The ground state is in the covalent subspace, so are the 2-photon states. Because of the non-alternancy, only fluoranthene will have non-zero dipole moment (4.22 Debye) in the ground state. The excitations to low-lying states in all molecules are shown in Fig. 2. In cases where the energy gap between levels in a molecule are small, we have ensured the linear independency of eigen states by computing the overlap of nearly degenerate eigen states. One common feature we note is that in all the molecules, the two-photon excitation is below the one-photon excitation, except in the case of fluoranthene, where the lowest excited singlet is in the B space and thus has a nonzero transition dipole. The lowest two-photon state in fluoranthene is about 0.2eV above the lowest one-photon state. In all other molecules, the lowest two-photon state is about 0.7 eV below the lowest one-photon state.

Hence except fluoranthene, none of the other molecules will be fluorescent by Kasha rule.<sup>40</sup> It is also reasonable to assume that the  $(2A - 1B)$  gap is a measure of the strength of electron correlation. We find it lowest in fluoranthene, implying that the effective electron correlations are

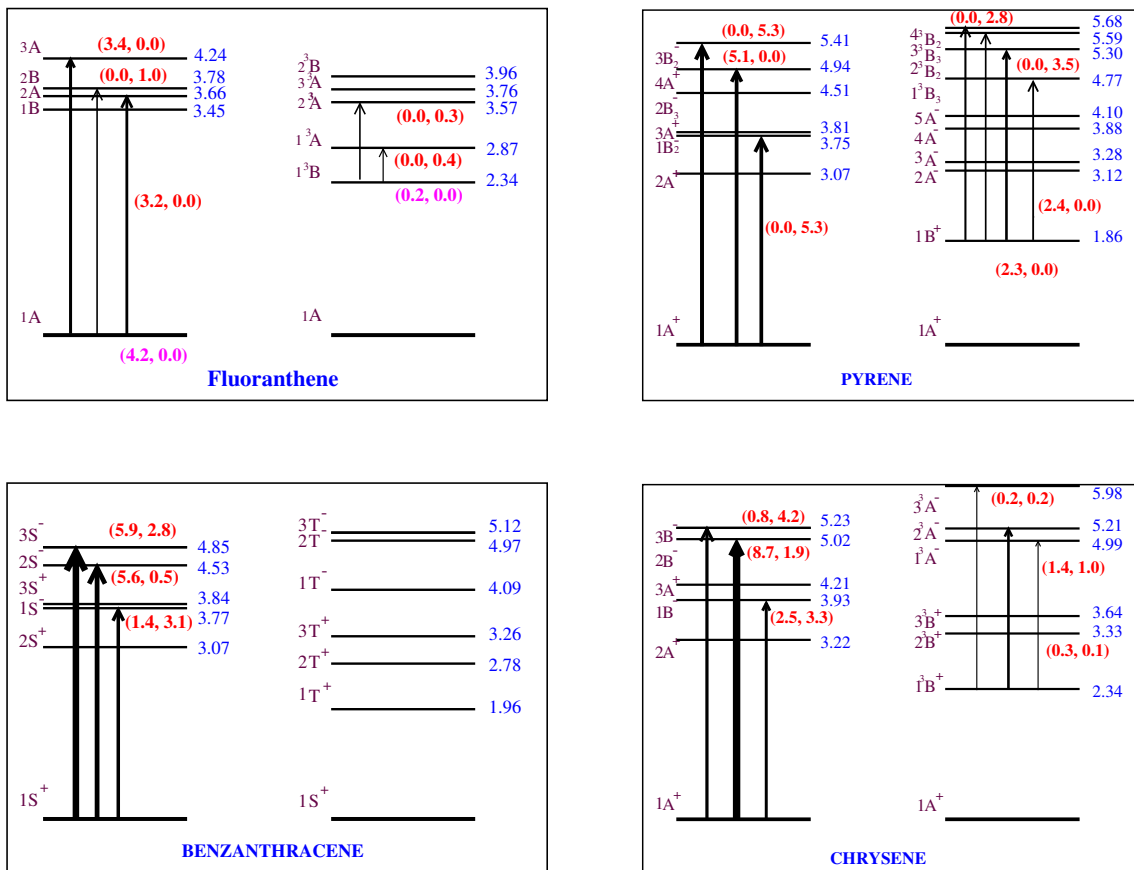


Figure 2: Low-lying excitation gaps for PAH molecules. Molecules are labelled in each box. The states shown to the left are singlets and those to the right are triplets. In the case of Fluoranthene, the symmetry labels were assigned from analyzing the eigenstates and confirmed from the polarization of the transition dipole. The transition dipoles are in Debye and energies are in eV. The spacing between labels is scaled to the magnitude of the gaps. The X and Y components of the transition dipoles are given in parenthesis and the thickness of the arrow indicates the strength of the transition. State labels with '+' and '-' superscripts correspond to 'covalent' and 'ionic' subspaces.

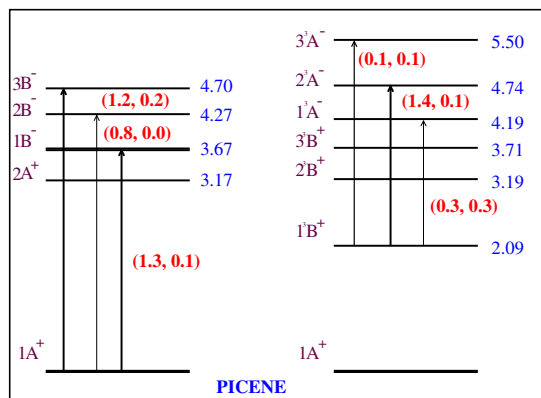
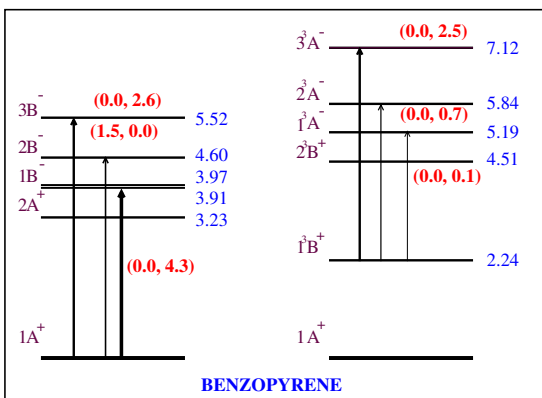
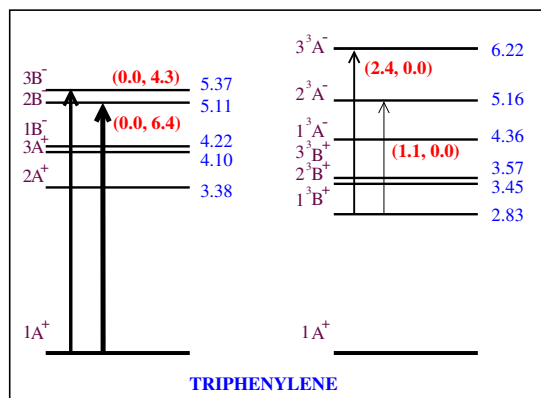
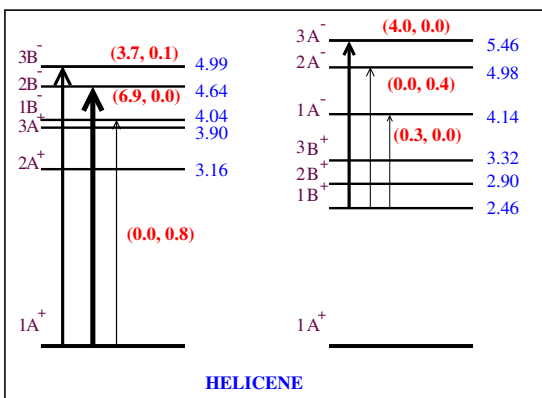


Figure 2 (contd.): Low-lying excitation gaps for the PAH molecules.

weakest in this system. Of the alternant systems, the weakest effective correlation is in picene and all the other systems show comparable effective correlation. The strongest optical absorption to 1Bu state is in benzopyrene and the weakest in chrysene. In many of these systems, we do observe strong excitations to higher singlet states. In Table 2, we give a comparison of experimental gaps with the theoretical gaps.<sup>41,42</sup> We find that our theoretical gaps compare very well with the experimental gaps. For pyrene molecule, we also find good agreement with the theoretical result of Basak et al obtained using the standard PPP parameters, taking quadruple CI basis.<sup>30</sup> Even the lowest two-photon gap compares well with their results from the standard parameters.<sup>31</sup> Triphenylene molecule having  $C_3$  symmetry shows two two-photon levels below  $B^-$  state. Here the excitation to the first  $B^-$  state is very weak and the second level is  $\approx 0.5$ eV higher than the experimental value.<sup>43,44</sup> In other cases also the experimental gaps are nearly 0.5 eV lower than the computed values, which can be attributed to solvent effects. In case of benzopyrene, the difference is slightly larger because the gap is obtained from the truncated CI basis within DMRG method.<sup>45</sup> Furthermore, since the molecule is not a quasi-one dimensional system (in contrast to picene), the excitation gap is slightly higher than the experimental gap.

We have given one-photon, two-photon and spin gaps of these molecules in Fig. 3. We find that in all the cases except pyrene and picene, the lowest triplet state is well above half of the singlet-singlet gap and hence none of the molecules are suitable for improving the solar cell efficiency via singlet fission. However, for pyrene and picene, since  $[E_{S1} - 2 \times E_{T1}]$  value is almost zero, these molecules can be tuned to have a favourable conditions for singlet fission, by substitution. In fact, B-N substituted pyrenes are shown to be possible candidate materials for singlet fission by Zeng et al.<sup>46</sup> In fluoranthene, pyrene, benzanthracene, benzopyrene and picene, the  $(2A - T_1)$  gap is  $\geq 1.0$  eV. However, triphenylene has the lowest  $2A - T_1$  gap of 0.5 eV, while the gap is 0.7 eV in helicene, and is 0.9 and 1.0 eV in chrysene and benzopyrene, respectively. We notice that the optical gap falls off rapidly from anthracene to pentacene (3.7 eV to 2.92 eV, see Table S1 in supporting information), whereas for phenacenes, it is slower

(4.3 eV for phenanthrene to 3.82 eV for picene). In the case of oligoacenes, the spin gap almost reaches zero, whereas for phenacenes, it is quite large, even in case of picene (1.95 eV).

**Table 2: Electronic excitation gap and singlet-triplet gaps in eV for PAH molecules. Numbers in the bracket are experimental gaps obtained from references shown as superscript. Except benzopyrene and picene other gaps are numerically exact. For benzopyrene and picene, the singlet-singlet and singlet-triplet gaps are obtained from DMRG studies.**

Molecule	Optical gap (Expt gap)	singlet- triplet gap
Fluoranthene	3.45 (3.46) <sup>41</sup>	2.34
Pyrene	3.75 (3.34) <sup>41,42</sup>	1.86
Benzanthracene	3.77 (3.23) <sup>41</sup>	1.96
Chrysene	3.95 (3.45) <sup>20</sup>	2.34
Helicene	4.04 (3.49) <sup>19</sup>	2.47
Triphenylene	5.11 (4.36) <sup>43,44</sup>	2.83
Benzopyrene	3.91 (3.38) <sup>45</sup>	2.28
Picene	3.82 (3.30) <sup>41</sup>	1.95

## Singlet State Properties

### Bond orders

We have computed the bond orders of the PAH molecules in various electronic states. The bond order between sites 'i' and 'j' is given by the expectation value of  $\hat{p}_{ij} = -\frac{1}{2} (\hat{E}_{ij} + \hat{E}_{ji})$  in the state of interest, where  $\hat{E}_{ij} = \sum_{\sigma} c_{i\sigma}^{\dagger} c_{j\sigma}$ . The larger the bond order, the shorter is the bond length and vice versa. Comparison of bond orders in a given excited state gives the propensity of a bond to shorten or lengthen with respect to the ground state bonds. At equilibrium, the ratio of bond length to bond order is expected to be the same for all bonds.

In Fig. 4, we have given the bond orders in the singlet ground state as well as the lowest one-photon excited state for all the PAHs we have studied. For comparison, we have given the bond

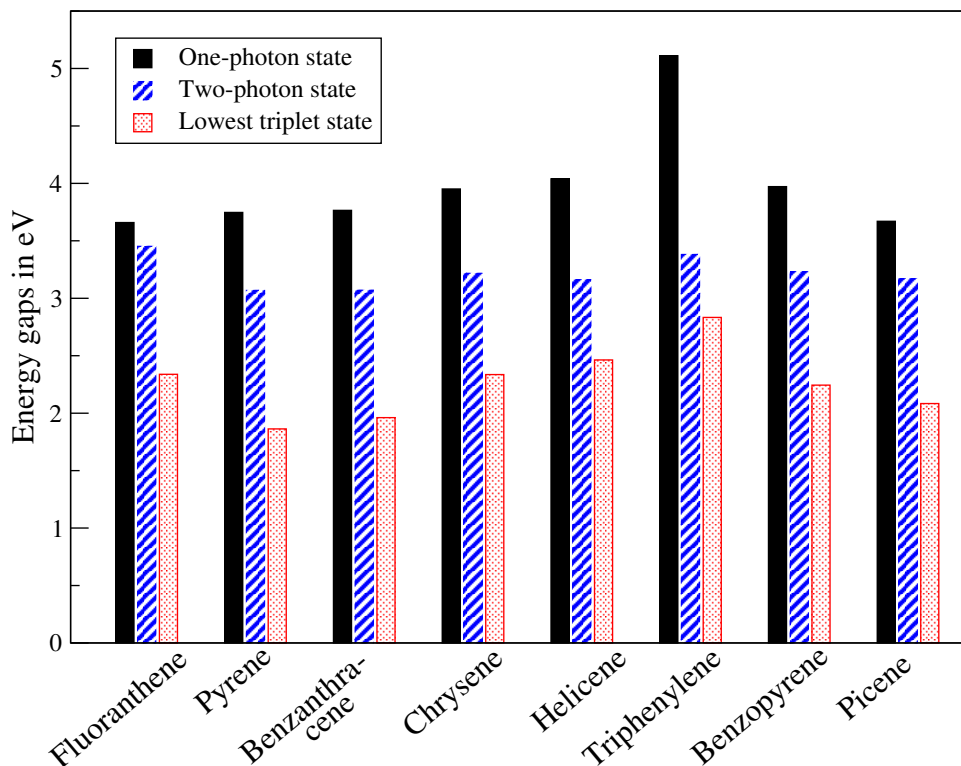


Figure 3: Energy gaps in eV, for one-photon state (black filled bar), two-photon state (blue hatched bar) and triplet states (red dotted bar) for PAHs molecules.

orders and spin densities of naphthalene, anthracene, phenanthrene and biphenyl molecules in supporting information (Fig. S1 and S2).

### Molecules with 16 $\pi$ -electrons (Fluoranthene and Pyrene)

In the ground state of fluoranthene, we note that the bond order of the bonds connecting the naphthalene unit and benzene unit are very small. This indicates that the two units are only weakly connected by the  $\pi$ -conjugation. The bond orders in the six membered rings are close to those of benzene in the Hückel model  $\sim 0.66$ , although bonds which are shared between rings have slightly lower bond order. In the optically excited state the bond connecting the benzene and naphthalene units become much stronger, indicating a contraction of the distance between the two units. The other bonds also show slightly smaller but nearly uniform bond

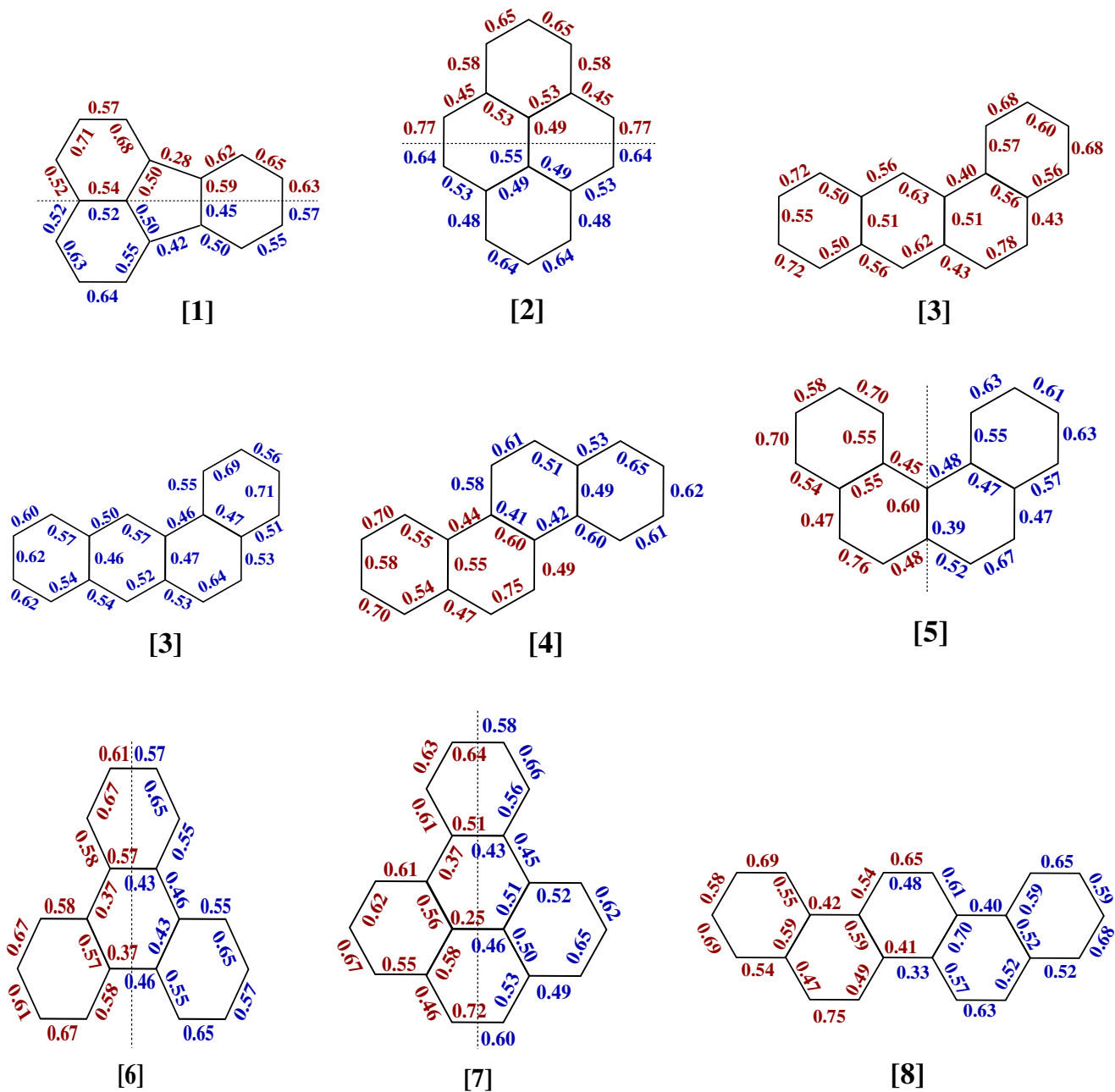


Figure 4: Bond orders in singlet ground state (in red) and in dipole allowed state (in blue). The numbering for molecules is as given in Figure 1.

orders, indicating ring expansion in the excited state. This also shows that the Stokes shift in the spectral lines will be large in this system. This is in conformity with large Stokes shift

observed experimentally, by Gusten and Heinrich.<sup>47</sup>

In pyrene, the bond orders in the ground state resemble those of biphenyl connected by two ethylenic units on either side, with alternate single and double bonds, rather than the bond orders of naphthalene connected by two propylenic units at the top and bottom. This is in accordance with the most possible resonance structures for pyrene. Compared to biphenyl, the central bond becomes stronger in pyrene (see Fig. S1). In the optically excited state, all the bond orders become more uniform. This shows that at equilibrium geometry, the molecule is not distorted much from the uniform bond lengths assumed in the calculations. We find a uniform expansion of rings in the optically excited state. We should expect the Stokes shift due to relaxation of the geometry in the excited state to be small as opposed to what is expected in fluoranthene.

### **Molecules with 18 $\pi$ -electrons (Benzanthracene, Chrysene, Helicine and Triphenylene)**

Benzanthracene molecule can be viewed as a phenyl ring attached either to an anthracene or to a phenanthrene. This is well reproduced by the bond order pattern in the ground state, where one of the two terminal rings have anthracenic like and the other two have phenanthrenic like bond orders (see SI Figure 1). In benzanthracene, the middle bond of armchair of the phenanthrenic moiety is the weakest while the bond opposite to that is the strongest. The ground state bond orders of both chrysene and helicene, again, resemble those of phenanthrene with a marginal change in bond orders. The middle bond of armchair of the phenanthrenic unit is the weakest and the bond opposite to that is the strongest, in accordance with the possible resonance structures. This is true even for helicene, where there are two weaker bonds at the arm chair, connecting the two naphthalenic unit. In both molecules, there is a slight enlargement of the rings in the excited state. The Stokes shift in these system are not expected to be large. The ground state bond orders in triphenylene molecule, correspond to three phenyl rings connected by a very weak bond (bond order is 0.37). The bond order pattern is reversed upon excitation, with the central ring having a more uniform and slightly stronger bonds compared to the ground



state geometry. Even in this molecule, the excited state geometry has more uniform bond orders. Once again the change in geometry from the ground state to the excited state is small, which leads us to expect small Stokes shift. Notice that the effect of non-conjugation in triphenylene is reflected in the excitation gap. Among all the PAHs we have studied, triphenylene has the largest optical gap and the singlet-triplet gap (see Table 2). Among 18  $\pi$ -electronic molecules, benzenanthracene has the lowest gap while chrysene and helicene have almost similar gap (3.95 eV and 4.04 eV, see Table 2) owing to their similarity in conjugation pattern.

### **Molecules with 20 (Benzopyrene) and 22 $\pi$ -electrons (Picene)**

Benzopyrene molecule has similar bond orders as those of triphenylene with an extra ethylenic unit connected at lower end of the molecule (see [7] in Fig. 4). Picene being a oligomer of phenanthrene, shows the ground state bond order similar to phenanthrene with minimal change in the bond orders of interior bonds. The change in equilibrium geometry from the ground to the excited state is not much, although the bond lengths in the excited states are slightly larger. Thus, even in picene, we should not expect large Stokes shift in the fluorescence.

## **Triplet State Properties**

### **Bond-Orders**

Fig. 5 gives bond orders of the PAH molecules in the lowest triplet and the lowest two photon states. In fluoranthene (1) the bond common to the two benzene rings becomes very weak and elongated while the peripheral bonds, except the one that connects the phenyl ring to the five membered ring, all have similar bond lengths at equilibrium. However the triplet bond orders show more alternation and only the bond connecting the benzene and naphthalene units stays

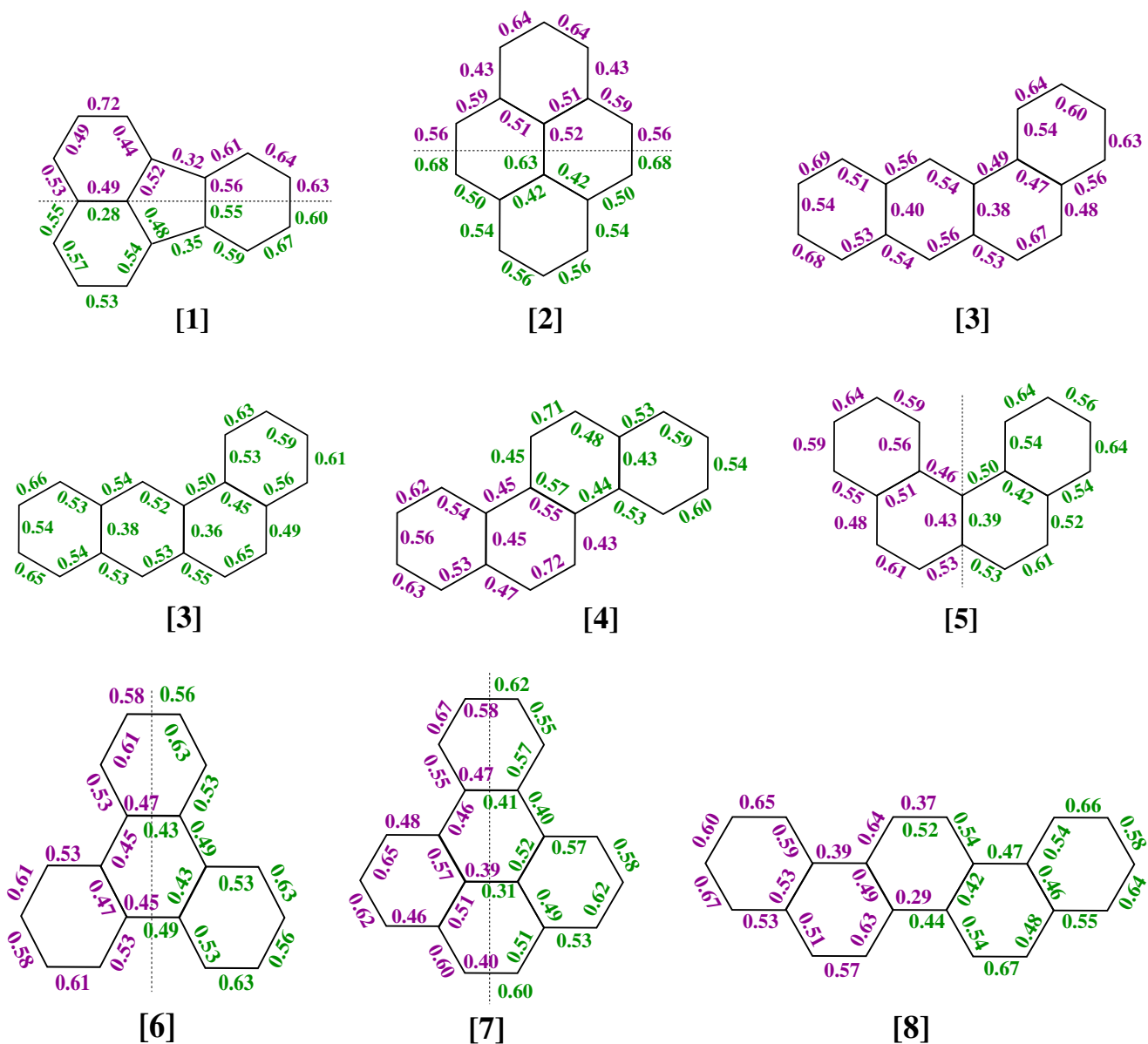


Figure 5: Bond orders in lowest triplet state (in magenta) and in two photon allowed state (in green). The numbering for molecules is as given in Figure 1.

elongated. In pyrene (2), bond orders in the triplet and two-photon allowed state show an opposite pattern. i.e. the bond orders are all nearly uniform in the naphthalenic unit in the triplet state and in biphenyl unit, they are alternating. On the other hand, in the two photon state, bonds are uniform in the biphenylenic unit whereas alternating in the naphthalenic unit. In benzan-

thracene (3), both the triplet and the two photon states have similar bond order patterns, with nearly uniform peripheral bonds and weaker inter-ring bonds. In chrysene as well as in helicene, both the triplet and the two photon states show bond alternation, although it is more pronounced in the two photon state. In helicene the bond lying at the  $C_2$  axis is the weakest bond both in the triplet state and two-photon allowed state (2A). In triphenylene (6), bond orders in both 2A and triplet states are similar and nearly uniform along the benzenic unit with a weaker central bond connecting the three phenyl rings. In benzopyrene (7), the interior bonds through which the  $C_2$  axis passes through, are weaker. In picene (8), the outer bonds have a marginal bond alternation in both the states, except the middle bond of the arm-chair of phenanthrenic units ( $0.35 \pm 0.05$ ). In the triplet state, the bonds connecting the two terminal naphthalene units to the central benzene ring are very weak (0.37 and 0.29), but only slightly weaker in the case of the 2A state (0.52 and 0.44) compared to other bonds.

## Spin Densities

Spin density at a site "i" is defined as the difference in charge density of up and down spins. i.e.  $\rho_i = \langle \Psi_k | a_{i\alpha}^\dagger a_{i\alpha} - a_{i\beta}^\dagger a_{i\beta} | \Psi_k \rangle = 2 \langle \Psi_k | S_z | \Psi_k \rangle$ . In Fig. 6 are given the spin densities in the lowest energy triplet state of the PAH molecules. We find large positive spin densities at the  $\alpha$  sites of the naphthalenic units of fluoranthene. There is slightly negative spin density at the sites common to the two benzene rings in the naphthalene unit. The total spin density is almost localised on the naphthalenic unit and spin density pattern resembles that of naphthalene (see supporting information Fig. S2). On the other hand, while isolated benzene has a significant spin density at each site (0.17), benzenic unit of fluoranthene has negligible spin density ( $< 0.02 \pm 0.01$ ). In pyrene, the largest positive spin densities are found at the  $\alpha$  sites (0.18) of biphenylinic unit followed by the  $\beta$  carbon atoms of naphthalenic unit (0.09). There is negative spin density at the two peripheral carbon atoms of biphenylinic unit ( $-0.05$ ) and all other carbon

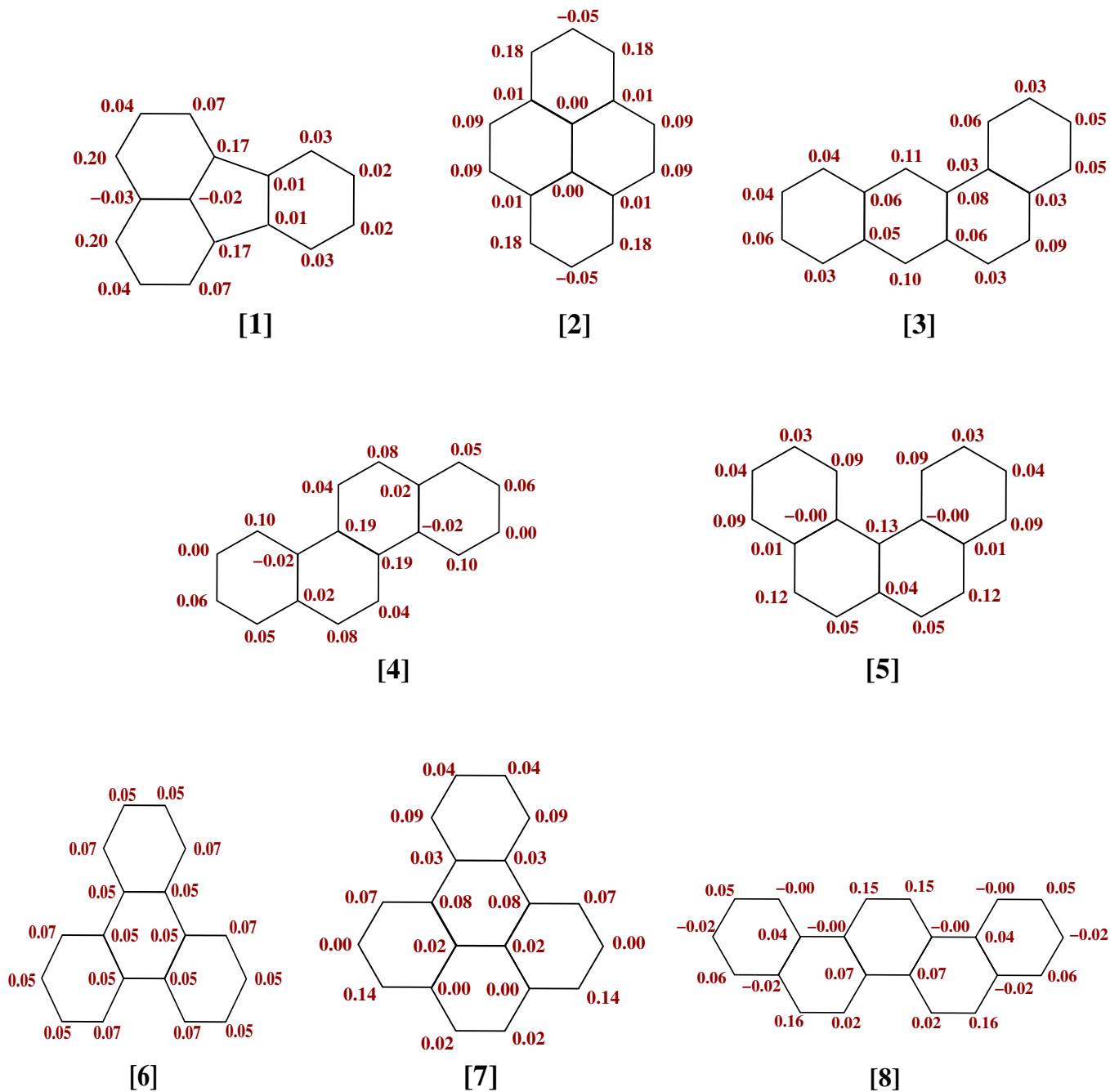


Figure 6: Spin densities in lowest triplet state are given in red color. The numbering of molecules are as given in Figure 1.

atoms have negligible spin densities.

Unlike the bond order pattern of benzanthracene, spin density pattern neither resembles that

of anthracene nor phenanthrenic unit. A uniform spin density ( $0.05 \pm 0.01$ ) is seen except at the  $\alpha$ - carbon atoms of anthracenic moiety (0.11). No negative spin density is observed in this molecule. Chrysene shows an opposite spin density pattern compared to other molecules. Here, the spin density is largest (0.19) at the two carbon atoms where two naphthelinic units are fused. It also shows negative spin densities at one of the adjacent sites followed by a large positive spin density (0.10 and 0.08) at the  $\alpha$  sites of naphthalenic units. On the other hand, in helicene almost all the  $\alpha$  sites have large positive spin densities ( $\sim 0.1$ ) and  $\beta$  sites have smaller spin densities. Triphenylene has a uniform spin density of 0.05 and 0.07 at alternate sites, with the central benzenic unit having a uniform spin density of 0.05, owing to its three-fold symmetry.

Benzopyrene has similar spin density pattern as that of triphenylene, with a pronounced alternation in spin densities at adjacent sites. The highest positive spin density of 0.14 is seen at the carbon atoms adjacent to the vinylenic bridge in benzopyrene. Picene molecule, on the other hand, has alternate positive and negative spin densities at the peripheral phenyl rings. There is also large positive spin densities (0.15) at four alpha carbon atoms of the interior naphthalenic units. The carbon atoms of the interior arm-chair have spin density of 0.07.

## Summary

In this paper we have studied the correlated electronic states of eight well known polycyclic aromatic hydrocarbons. From energetics, we find that in all these molecules, the one-photon state is above the two photon state. Hence none of these molecules are expected to be fluorescent. The optical gap obtained from our study agree well with the experimental gaps. The singlet-triplet gap in all the molecules is also quite large and does not satisfy the requirements for singlet fission. The bond orders show that the equilibrium geometries of all the states are nearly the same as assumed in the calculations. Thus, we expect small Stokes shifts in fluorescence. The

spin densities in the triplet state are mostly confined to the  $\alpha$  sites of the naphthalenic units in the molecules. Most molecules show very small negative spin densities at a few sites and often all the sites have only positive spin densities.

## Supporting Information Available

The following files are available free of charge. We have given the following table and figures:

- i) A Table for electronic excitation gap and singlet-triplet gaps for PAH molecules - naphthalene, anthracene and phenanthrene.
- ii) A figure for bond orders for the lowest singlet and triplet states for naphthalene, anthracene, phenanthrene and biphenyl.
- iii) A figure containing spin densities of the lowest triplet states for naphthalene, anthracene, phenanthrene and biphenyl.

## Acknowledgement

Y. A. P. thanks Disha programme for women in Science (DST0128), Department of Science and Technology, Government of India, for financial support.

## References

- (1) Salem, L.; *Molecular Orbital Theory of Conjugated Systems*, W. A. Benjamin: New York, (1966); Chapter 4.
- (2) Kuwajima, S.; Soos, Z. G. Enhanced Ring Current of Charged Annulenes, *J. Am. Chem. Soc.*, **1986** *108*, 1707-1708.

- (3) Gomes, J. A. N. F.; Mallion, R. B. Aromaticity and Ring Currents, *Chem. Rev.*, **2001**, *101*, 1349-1384.
- (4) Zhang, Y.; Sheng, W.; Li, Y. Dark Excitons and Tunable Optical Gap in Graphene Nanodots, *Phys. Chem. Chem. Phys.*, **2017**, *19*, 23131-23137.
- (5) Hai, X.; Feng, J.; Chen, X.; Wang, J. Tuning the Optical Properties of Graphene Quantum Dots for Biosensing and Bioimaging, *J. Mater. Chem. B*, **2018**, *6*, 3219-3234.
- (6) Chen, S.; Ullah, N.; Wang, T.; Zhang, R. Tuning the Optical Properties of Graphene Quantum Dots by Selective Oxidation: a Theoretical Perspective, *J. Mater. Chem. C*, **2018**, *6*, 6875-6883.
- (7) Wettstein, C.M.; Bonafe, F. P.; Oviedo, M. B.; Sanchez, C. G. Optical Properties of Graphene Nanoflakes: Shape Matters, *J. Chem. Phys.*, **2016**, *144*, 224305.
- (8) Sharma, SRKC Y.; Bandyopadhyay, A.; Pati, S. K. Structural Stability, Electronic, Magnetic, and Optical Properties of Rectangular Graphene and Boron Nitride Quantum Dots: Effects of Size, Substitution, and Electric Field, *J. Phys. Chem. C*, **2013**, *117*, 23295-23304.
- (9) Alam, Sk. M.; Ananthanarayanan, A.; Huang, L.; Lim, K. H.; Chen, P. Revealing the Tunable Photoluminescence Properties of Graphene Quantum Dots, *J. Mater. Chem. C*, **2014**, *2*, 6954-6960.
- (10) Geethalakshmi, K. R.; Yong Ng Y.; Crespo-Otero, R. Tunable Optical Properties of OH-Functionalised Graphene Quantum Dots *J. Mater. Chem. C*, **2016**, *4*, 8429-8438.
- (11) Mitsuhashi, R.; Suzuki, Y.; Yamanari, Y.; Mitamura, H.; Kambe, T.; Ikeda, N.; Okamoto, H.; Fujiwara, A.; Yamaji, M.; Kawasaki, N.; Maniwa, Y.; Kubozono, Y. Superconductivity in Alkali Metal Doped Picene, *Nature*, **2010**, *464*, 76-79.

- (12) Xue, M.; Cao, T.; Wang, D.; Wu, Y.; Yang, H.; Dong, X.; He, J.; Li, F.; Chen, G. F. Superconductivity Above 30 K in Alkali-Metal-Doped Hydrocarbon, *Sci. Rep.*, **2012**, *2*, 389.
- (13) Artioli, G. A.; Hammerath, F.; Mozzati, M. C.; Carretta, P.; Corana, F.; Mannucci, B.; Margadonna, S.; Malavasi, L. Superconductivity in Sm-Doped [n] Phenacenes (n =3,4,5), *Chem. Commun.*, **2015**, *51*, 1092-1095.
- (14) Nakagawa, T.; Yuan, Z.; Zhang, J.; Yussenko, K. V.; Drathen, C.; Liu, Q.; Margadonna, S.; Jin, C. Structure and Magnetic Property of Potassium Intercalated Pentacene: Observation of Superconducting Phase in  $K_xC_{22}H_{14}$ , *J. Phys.: Condens. Matter*, **2016**, *28*, 484001.
- (15) Allamandola, L. J.; Sandford, S. A.; Wopenka, B. Interstellar Polycyclic Aromatic Hydrocarbons and Carbon in Interplanetary Dust Particles and Meteorites, *Science*, **1987**, *237*, no. 4810, 56-59.
- (16) Allamandola, L. J.; Tielens, A. G. G. M.; Barker, J. R., Polycyclic Aromatic Hydrocarbons and the Unidentified Infrared Emission Bands - Auto Exhaust Along the Milky Way, *Astrophys. J. Part II*, **1985**, *290*, L25-L28.
- (17) d'Hendecourt L.; Ehrenfreund P. Spectroscopic Properties of Polycyclic Aromatic Hydrocarbons (PAHs) and Astrophysical Implications, *Adv. Space Res.*, **1997**, *19*, 1023-1032.
- (18) Salama, F.; Galazutdinov, G. A.; Krelowski, J.; Biennier, L.; Beletsky, Y.; Song, I-O. Polycyclic Aromatic Hydrocarbons and the Diffuse Inetestellar Bands: A Survey, *Astrophys. J.*, **2011**, *728*, 154.
- (19) Palewska, K.; Ruziewicz, Z.; Chojnacki H.; Meister, E. C. High-resolution Electronic Spectra of Tetrahelicene and Hexahelicene in Low-Temperature Polycrystalline Matrices, *Chem. Phys.*, **1992**, *161*, 437-445.



- (20) Hussain, M. M. Measurement and Theoretical Characterization of Electronic Absorption Spectrum of Neutral Chrysene and Its Positive Ion in  $H_3BO_3$  Matrix, *Spectrochim. Acta A*, **2007**, *68*, 156-164.
- (21) Canuto, S.; Zerner, M. C.; Diercksen, G. H. F. Theoretical Studies of the Absorption Spectra of Polycyclic Aromatic Hydrocarbons, *Astrophys. J. Part I*, **1991**, *377*, 150-157.
- (22) Ping Du, Salama, F.; Loew, G. H. Theoretical Study of the Electronic Spectra of a Polycyclic Aromatic Hydrocarbon, Naphthalene, and its Derivatives, *Chem. Phys.*, **1993**, *173*, 421-427.
- (23) Langhoff, S. R. Theoretical Infrared Spectra for Polycyclic Aromatic Hydrocarbon Neutrals, Cations, and Anions, *J. Phys. Chem.*, **1996**, *100*, 2819-2841.
- (24) Mallocci, G.; Mulas, G.; Joblin, C. Electronic Absorption Spectra of PAHs up to Vacuum UV Towards a Detailed Model of Interstellar PAH Photophysics, *Astron. Astrophys.*, **2004**, *426*, 105117.
- (25) Filipp, F.; Reinhart, A. Adiabatic Time-Dependent Density Functional Methods for Excited State Properties, *J. Chem. Phys.*, **2002**, *117*, 7433-7447.
- (26) Hammonds, M.; Pathak, A.; Sarre, P. J. TD-DFT Calculations of Electronic Spectra of Hydrogenated Protonated Polycyclic Aromatic Hydrocarbon (PAH) Molecules: Implications for the Origin of the Diffuse Interstellar Bands, *Phys. Chem. Chem. Phys.*, **2009**, *11*, 4458-4464.
- (27) Cocchi, C.; Prezzi, D.; Ruini, A.; Caldas, M. J.; Molinari, E. Anisotropy and Size Effects on the Optical Spectra of Polycyclic Aromatic Hydrocarbons, *J. Phys. Chem. A*, **2014**, *118*, 6507-6513.

- (28) SeyedAbdolreza, S.; Yong Z.; Sun, K. A Theoretical Study on the Vibrational Spectra of Polycyclic Aromatic Hydrocarbon Molecules with Aliphatic Side Groups, *Astrophys. J.*, **2015**, *801*, 34.
- (29) Aryanpour, K.; Roberts, A.; Sandhu, A.; Rathore, R.; Shukla A.; Mazumdar, S. Sub-gap Two-Photon States in Polycyclic Aromatic Hydrocarbons: Evidence for Strong Electron Correlations, *J. Phys. Chem. C*, **2014**, *118*, 3331-3339.
- (30) Basak, T.; Chakraborty, H.; Shukla, A. Theory of Linear Optical Absorption in Diamond-Shaped Graphene Quantum Dots, *Phys. Rev. B.*, **2015**, *92*, 205404.
- (31) Basak, T.; Basak T.; Shukla, A. Electron Correlation Effects and Two-Photon Absorption in Diamond-Shaped Graphene Quantum Dots, *Phys. Rev. B.*, **2018**, *98*, 035401.
- (32) Lykos, P. G. and Parr, R. G. On the  $\pi$  Electron Approximation and Its Possible Refinement, *J. Chem. Phys.*, **1956**, *24*, 1166-1173.
- (33) Pariser, R.; Parr, R. G. A Semi-Empirical Theory of the Electronic Spectra and Electronic Structure of Complex Unsaturated Molecules. II, *J. Chem. Phys.*, **1953**, *21*, 767-776.
- (34) Pople, J. A., The Electronic Spectra of Aromatic Molecules II: A Theoretical Treatment of Excited States of Alternant Hydrocarbon Molecules Based on Self-Consistent Molecular Orbitals, *Proc. Phys. Soc. A*, **1955**, *68*, 81-89.
- (35) Ohno, K. Some Remarks on the Pariser-Parr-Pople Method, *Theor. Chim. Acta*, **1964**, *2*, 219-227.
- (36) Soos, Z. G.; Ramasesha, S. Valence Bond Approach to Exact Nonlinear Optical Properties of Conjugated Systems, *J. Chem. Phys.*, **1989**, *90*, 1067-1076.
- (37) Ramasesha, S.; Soos, Z. G. Diagrammatic Valence-Bond Theory for Finite Model Hamiltonians, *Int. J. Quantum Chem.*, **1984**, *25*, 1003-1021.

- (38) Ramasesha, S.; Soos, Z. G. Symmetry Adaptation of Correlated States in the Valence Bond Basis, *J. Chem. Phys.*, **1993**, *98*, 4015-4022.
- (39) Rettrup, S. An iterative Method for Calculating Several of the Extreme Eigensolutions of Large Real Non-Symmetric Matrices, *J. Comp. Phys.*, **1982**, *45*, 100-107.
- (40) Kasha, M.; Characterization of Electronic Transitions in Complex Molecules, *Discuss. Faraday Soc.*, **1950**, *9*, 14-19.
- (41) Clarence, K. Jr. The Longest Wavelength Band in the Electronic Spectra of Polycyclic Aromatic Hydrocarbons for Analytical Use, *Appl. Spectr.*, **1959**, *13*, 15-25.
- (42) Sun, Y. P. Excitation Wavelength Dependence of Pyrene Fluorescence in Supercritical Carbon Dioxide. Evidence for a Supercritical Solvent-Assisted Solute-Solute Clustering Mechanism *J. Am. Chem. Soc.*, **1993**, *115*, 3340-3341.
- (43) Hall, R. D.; Valeur, B.; Weber, G. Polarization of the Fluorescence of Triphenylene: a Planar Molecule with Threefold Symmetry, *Chem. Phys. Lett.*, **1985**, *116*, 202-205.
- (44) Tanikawa, T.; Saito, M.; Guo, J. D.; Nagase, S. Synthesis, Structures and Optical Properties of Trisilasumanene and its Related Compounds, *Org. Biomol. Chem.*, **2011**, *9*, 1731-1735.
- (45) Schwarz F. P.; Wasik, S. P. Fluorescence Measurements of Benzene, Naphthalene, Anthracene, Pyrene, Fluoranthene, and Benzo[e]pyrene in Water, *Analytical Chem.*, **1976**, *48*, 525-527.
- (46) Zeng, T; Mellerup, S. K.; Yang, D.; Wang, X.; Wang, S.; Stampelcoskie, K. Identifying (BN)<sub>2</sub> pyrenes as a New Class of Singlet Fission Chromophores: Significance of Azaborine Substitution, *J. Phys. Chem. Lett.*, **2018**, *9*, 2919-2927.

- (47) Gusten, H.; Heinrich, G. Photophysical Properties of Fluoranthene and its Benzo Analogues, *J. Photochem.*, **1982**, *18*, 9-17.